THE JOURNAL OF PHYSICAL CHEMISTRY C
A JOURNAL OF THE AMERICAN CHEMICAL SOCIETY

pubs.acs.org/JPCC

Article

Tunable Magnetic and Electronic Properties of the 2D CoO_2 Layer

Li Liang, Shiqiao Du, Lili Wang, Zheng Liu,* Jian Wu,* and Shunhong Zhang*

Cite This: *J. Phys. Chem. C* 2021, 125, 873–877

Read Online

ACCESS | Metrics & More | Article Recommendations | Supporting Information

ABSTRACT: By performing first-principles calculations, we find that the predominant spin exchange of a hexagonal CoO_2 layer is in proximity to the ferromagnetic-to-antiferromagnetic transition point. Its magnetic ground state can be easily altered by, e.g., substrate dielectricity and strain. In addition, the dopability of a stack of CoO_2 layers is found to sensitively depend on the interlayer distance, which not only renders effective manipulation of the electronic property but also reveals an important intercalation effect in related bulk materials.

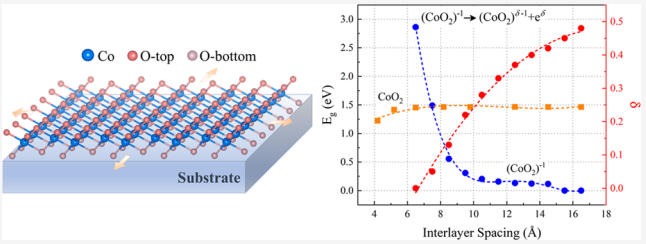

INTRODUCTION

The hexagonal CoO_2 layer is the building block of lithium or sodium cobalt oxides. These materials show excellent thermal and ionic transport properties, which have found important applications in thermoelectricity[1,2] and rechargeable batteries.[3−5] The discovery of superconductivity in hydrated $Na_xCoO_2{\cdot}yH_2O (y \approx 1.3)$[6] put forth the CoO_2 layer as a new platform to study strong correlation physics in parallel to the CuO_2 layer in high T_c superconducting cuprates, which generated a surge of investigations in the prepnictide era.[7−11] A novel challenge is to account for strong correlation, geometry frustration, and the complicated effects induced by the intercalated elements simultaneously.[7,9,12,13]

In the past years, both the CuO_2 monolayer[14,15] and the FeSe monolayer[16] have been successfully grown by molecular beam epitaxy (MBE), which renders an unprecedented transparent study of the essential building blocks of strongly correlated materials. Some preliminary MBE data have been collected, suggesting that a CoO_2 monolayer can be fabricated similarly.[17] Free from the intercalation complications, a high-quality MBE CoO_2 monolayer is not only of technical interest but also expected to clarify the intrinsic strong correlation physics. At the same time, epitaxial Na_xCoO_2 thin films have already been grown by pulsed laser deposition.[18]

In this paper, we predict efficient tunability of the magnetic and electronic properties of the two-dimensional (2D) CoO_2 layer based on first-principles calculations. On the one hand, we find that the magnetic interactions in a CoO_2 layer can be nicely described by a nearest-neighbor Heisenberg model. The spin exchange parameter is in proximity to a ferromagnetic (FM)-to-antiferromagnetic (AFM) transition point, and thus the magnetic ground state can be manipulated by some external knobs, such as substrate dielectricity and strain. On the other hand, dopability of a stack of CoO_2 layers is found to sensitively depend on the interlayer spacing. In particular, when the interlayer spacing increases from ∼5 Å, as in bulk Na_xCoO_2, to ∼10 Å, as in H_2O-intercalated Na_xCoO_2, the electron-doped $(CoO_2)^-$ layer undergoes a spontaneous overflow of electrons, which forms interlayer conducting channels.

COMPUTATIONAL METHODS

Our calculations are performed using the Vienna *Ab initio* Simulation Package (VASP).[19] The projector augmented wave method[20] is employed to deal with ions and core electrons, while the exchange−correlation functional of the valence electrons employs the generalized gradient approximation parametrized by Perdew, Burke, and Ernzerhof (PBE).[21] The cutoff energy of plane-wave basis is 600 eV. The structures are fully relaxed until the force is less than 0.01 eV/Å. The localized Co 3d-electrons are treated with the rotational-invariant DFT+U correction.[22]

RESULTS AND DISCUSSION

Figure 1a schematically shows an epitaxially grown CoO_2 monolayer, structurally similar to the T-phase transition metal dichalcogenides (TMD), in which each Co atom is located at the center of an octahedron formed by six O atoms. This 2D sheet tiled by edge-sharing CoO_6 octahedra is also structurally similar to bulk CoO_2, the end member of a Na_xCoO_2 compound. The relaxed lattice constant is 2.845 Å, close to that of the bulk hexagonal phase (2.822 Å).[23] In the bulk Na_xCoO_2 compound, such CoO_2 layers are stacked in an ABC sequence, with Na ions intercalated in the interlayer space. Because previous studies[24] have revealed that the

Received: August 28, 2020
Revised: December 20, 2020
Published: January 4, 2021

https://dx.doi.org/10.1021/acs.jpcc.0c07847
J. Phys. Chem. C 2021, 125, 873–877

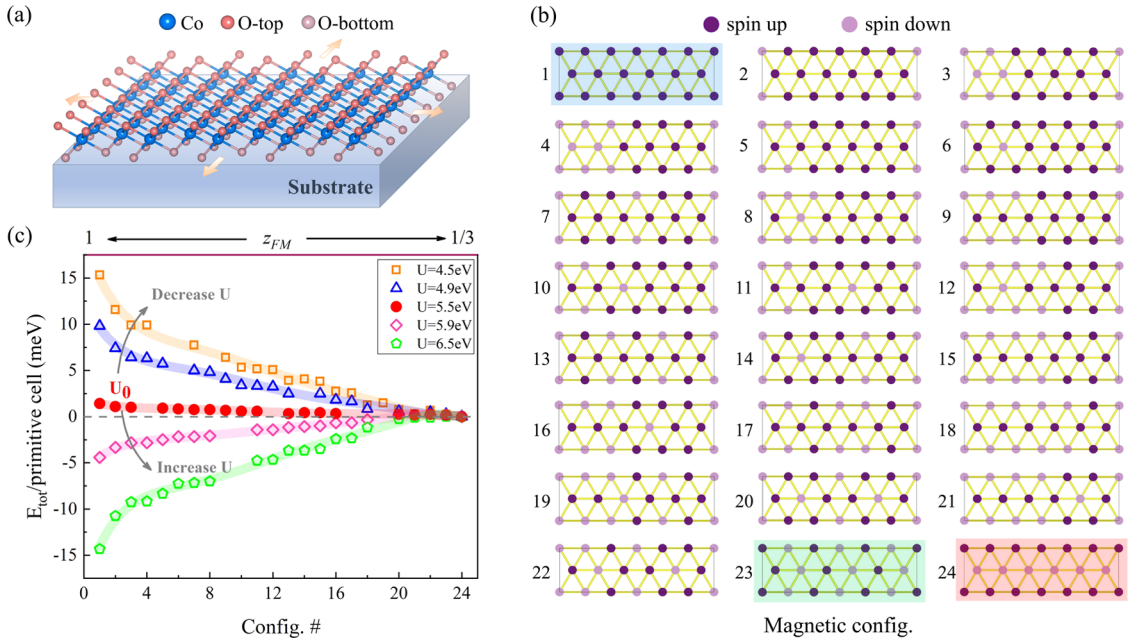

Figure 1. (a) Schematics of an epitaxial 2D CoO_2 layer; (b) calculated magnetic configurations in the rectangular supercell formed by the Co atoms; and (c) DFT+U energy per primitive cell as a function of the magnetic configuration. The stripe AFM configuration (#24) is chosen as the energy reference, and z_{FM} denotes the average percentage of the FM bonds.

interlayer spacing has a more pronounced influence on the properties, here, for simplicity, we use a unit cell with only one monolayer for simulation and the bulk limit is approached by reducing the vacuum distance normal to the basal plane of the monolayer. We have also inspected the effect of a more complex stacking sequence such as ABC-stacking[25] and found the predicted physics still holds (Figure S1). In the 2D limit, monolayer CoO_2 is simulated in a freestanding form whose dynamical and thermal stabilities are confirmed by our phonon spectra calculation and *ab initio* molecular dynamics simulation, respectively (Figure S2), and the substrate effects on its correlation strength and lattice constants are investigated by altering the +U parameter and the in-plane strain, respectively.

We first benchmark our calculation with the pioneering DFT +U study on pristine CoO_2 layers done by Louie's group in 2004.[10] This previous calculation was mainly designed to reflect the three-dimensional (3D) bulk properties by employing an interlayer spacing d = 6.5 Å, located between the values of the unhydrated and hydrated Na_xCoO_2 samples. Using the same structural and +U parameters (U_0 = 5.5 eV; J_0 = 0.9 eV), the insulating band structure under the FM spin configuration can be nicely reproduced. The magnetic moment per unit cell is 1 μ_B, indicating a low-spin S = 1/2 state of the Co^{4+} ion. Further increasing d to 16.5 Å to simulate the 2D limit results in little change, indicating that the interlayer coupling is already weak enough at d = 6.5 Å. We note that previous experiments showed that such a large interlayer spacing could no longer be held in the 3D bulk with depleted intercalated ions, resulting in a transition from a quasi-2D insulator to a 3D metal.[26] In this respect, the 2D physics associated with the pure CoO_2 layers can only be reached in an epitaxial form.

The magnetic structure of the pristine CoO_2 layer remains unclear. We thus extend the calculations from a single FM spin configuration to over 20 different spin configurations in a large rectangular supercell formed by the Co atoms (Figure 1b). The magnetic moment localized at each Co ion is ~1 μ_B for all of the considered spin configurations. We calculate their total energies using the structure relaxed from the FM configuration. These spin configurations are sorted with respect to the average percentage of the FM bonds (z_{FM}): z_{FM} = 1 corresponds to the FM configuration (#1) and z_{FM} = 1/3 corresponds to a stripe AFM configuration (#24). Note that on a triangular lattice, it is impossible to reach z_{FM} = 0 in a classical picture. It is surprising to notice that the total energies are almost degenerate at U_0 = 5.5 eV, as if the spins are largely free (Figure 1c). We exclude geometry frustration or symmetry as the origin because the degeneracy can be removed by selecting different +U parameters (Figure 1c). Specifically, decreasing U makes the FM bond energetically unfavored, whereas increasing U acts oppositely.

Under a given U, the over 20 DFT+U energies can be nicely fitted by a single-parameter Heisenberg model $H = -J_H \sum_{\langle i,j \rangle} \boldsymbol{S}_i \cdot \boldsymbol{S}_j$, in which $\langle i, j \rangle$ labels the nearest pair of two Co^{4+} ions, $\boldsymbol{S}$ is the 1/2 spin operator, and J_H is the effective spin exchange. The correlation coefficient R^2 is above 0.987, and this good fitting quality remains even when some spin configurations generated in other supercells are included (Figure S3). As shown in Figure 2, the fitted J_H shows a strong linear dependence on U, within the tested range. This outcome is understood as a competition between the FM direct exchange and AFM superexchange, both of which arise from the Coulombic interactions associated with Co 3d-orbitals, and importantly, U_0 = 5.5 eV happens to be around the balance point. Specifically, the FM direct exchange mainly arises from the d-shell overlap of two Co ions, which is primarily an atomic property largely insensitive to the U_0 parameter. On the other hand, the AFM superexchange is associated with a virtual transition between Co d^5 and d^6 states, and scales as $1/U_0$. Therefore, the balance between the FM and AFM exchange can be upset by tuning the U_0 strength. It is worth mentioning that unlike the magnetic ground state, the insulating gap is quite stable under different +U parameters (Figure S4).

https://dx.doi.org/10.1021/acs.jpcc.0c07847
J. Phys. Chem. C 2021, 125, 873−877

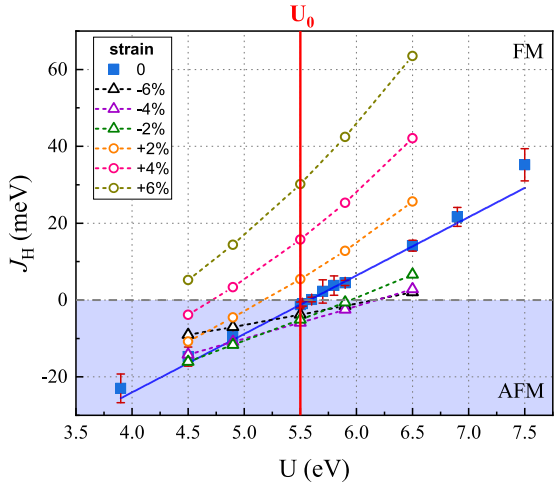

Figure 2. Fitted nearest-neighbor Heisenberg exchange as a function of U and strain. The error bars on the zero-strain data points indicate the root-mean-square of the residual from the sampled magnetic configurations.

We note that in the previous calculations of bulk Na_xCoO_2, while the employed J values are close, the U values associated with Co 3d-oribtals vary from 3 to 5.5 eV.[10,13,27,28] Our own U-value calculation based on the linear response approach[29] gives a very similar result to ref 10 and increasing the interlayer distance to reach the 2D limit only slightly enhances U to 5.6 eV. In practice, the effective Coulombic repulsion of an epitaxial thin film can be modulated by the dielectricity of the substrate and charge doping. This tunability has already been demonstrated experimentally for iron-based superconductors.[30,31] The strong dependence of J_H on U and its proximity to the sign-changing point renders effective tunability of the magnetic property of the CoO_2 layer. As a further demonstration, we show in Figure 2 that the FM-to-AFM transition can also be realized by applying a few percents of in-plane biaxial strain under fixed U. The overall trend is that the compressive strain pushes J_H to the AFM side and slightly decreases the slope of $J_H(U)$, whereas the tensile strain acts oppositely.

We now turn to consider charge doping into the 2D CoO_2 layers. We first show that without doping, the insulating gap is nearly unchanged under different magnetic configurations (Figure 3a). In combination with the fact that the number of valence electrons per primitive lattice cell is odd, these results naturally coincide with the common perception that the pristine CoO_2 insulating state is of the Mott nature. The doping calculation below is performed within a primitive cell under the FM configuration.

For bulk samples, a high doping level close to one electron per Co can be achieved by Li and Na intercalation, reaching a nominal $(CoO_2)^-$ stoichiometry. In ref 10, this limit is simulated by adding one electron per primitive lattice cell and a compensating uniform positive charge background. Following the same recipe and using an interlayer spacing d = 6.5 Å

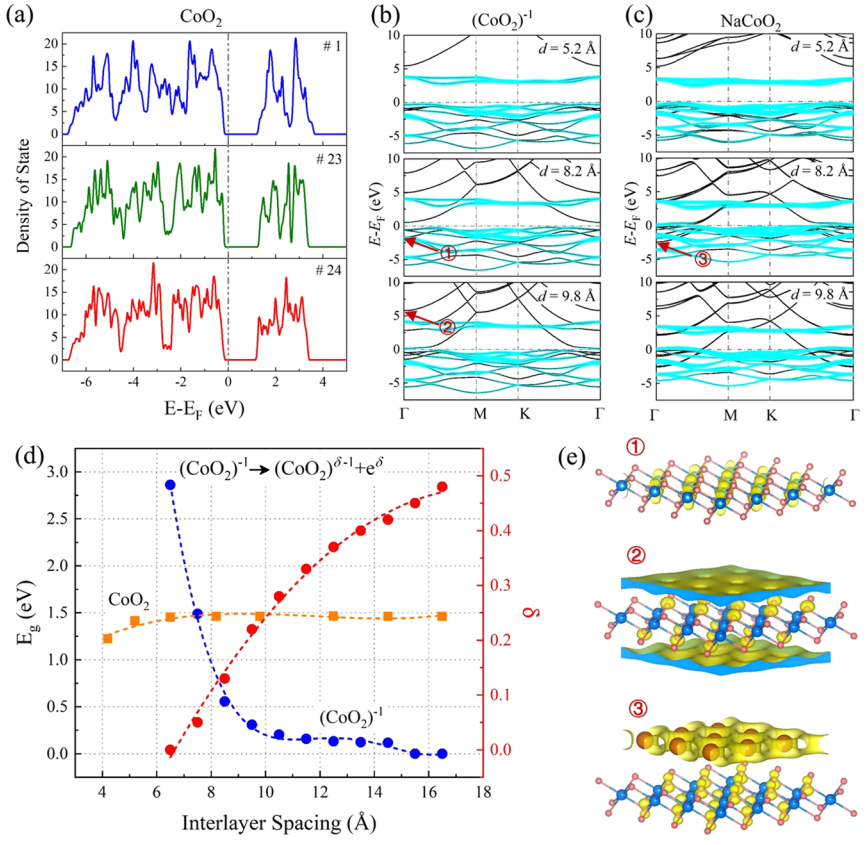

Figure 3. (a) Density of states (DOS) of an undoped CoO_2 layer under different magnetic configurations; the band structure of (b) $(CoO_2)^-$ and (c) $NaCoO_2$ with varying interlayer spacing d. The thickness of the cyan fat lines represents the weights of Co-d orbitals; (d) energy gap dependence of the interlayer distance for CoO_2 (orange) and $(CoO_2)^-$ (blue) layers and interlayer charge δ of $(CoO_2)^-$ (red) as a function of the interlayer distance; and (e) charge distribution of selected electronic states as labeled in (b) and (c).

https://dx.doi.org/10.1021/acs.jpcc.0c07847
J. Phys. Chem. C 2021, 125, 873−877

(the in-plane lattice constant is relaxed and found to be almost invariant upon doping), again, we can nicely reproduce the nonmagnetic band insulating state containing an even number of valence electrons. However, in contrast to the undoped case, where increasing d leads to little change, the band structure of $(CoO_2)^-$ varies dramatically as the layers are further separated apart. We should point out that the charge neutrality has been restored by the positive charge background. Therefore, this variation is not related to the long-range Coulombic potential of charged systems. As shown in Figure 3b, the general trend is the downward shift of some free-electron-like bands. An examination on the charge distribution of these bands confirms that they are interlayer states (Figure 3e). When these interlayer bands intersect the Fermi level, a fraction of the original Co d-bands becomes unfilled, signifying a spontaneous overflow of the electrons to the interlayer space. When the interlayer space shrinks, these interlayer electrons are squeezed back to the CoO_2 layers. The emergence of low-energy interlayer states significantly reduces the energy gap (Figure 3d), leading to interlayer conducting channels. In analogy to the formation of an electride,[32,33] this overflow can be viewed as a decomposition of $(CoO_2)^-$ into $(CoO_2)^{\delta-1} + e^{\delta}$, and δ can be used as a measure of the dopability of the CoO_2 layer (Figure 3d).

Based on these results, we conclude that the dopability of CoO_2 layers sensitively depends on the interlayer spacing. It is most difficult to dope a CoO_2 monolayer to the Co^{3+} limit, but when these monolayers stack up, this doping bottleneck will be gradually released as the film thickness approaches to the 3D limit. To ensure that these results are not artifacts of the compensating charge background, we have also calculated the band structure of $NaCoO_2$ with a manually increased distance between the Na layer and the CoO_2 layer (Figure 3c). The same band evolution is observed: when there is plenty of interlayer spaces, fewer electrons can be transferred from Na to the CoO_2 layer, and some free-electron-like interlayer bands emerge.

This observation suggests the interlayer states as a potentially important ingredient to understand the superconductivity in hydrated Na_xCoO_2.[66] A prominent effect of the intercalated water molecules is to double the distance between the CoO_2 layers from about 5 to 10 Å. According to our results, the interlayer states already sink below the Fermi level under such a large interlayer spacing. A parallel can be drawn with graphite intercalation compounds (GIC). Many experiments have demonstrated that intercalating alkali or alkali earth elements can induce superconductivity in graphite.[34] Similar interlayer states are also noticed in calculation and are shown to have a close correlation with T_c.[35] We should also emphasize that the strong correlation nature of the CoO_2 layer is distinct from the graphene layers. The relative role of the Co 3d-electrons and the interlayer states and the superconducting pairing mechanism still require further investigations.

CONCLUSIONS

In conclusion, by performing first-principles calculations, we reveal interesting magnetic and electronic properties of the 2D CoO_2 layer, which is the building block of lithium or sodium cobalt oxides. We first show that Co−Co magnetic interaction in a neutral CoO_2 monolayer can be well mapped to a nearest-neighbor Heisenberg model. The exchange parameter J_H is in proximity to the ferromagnetic-to-antiferromagnetic transition point, therefore the ground state magnetic configuration can be conveniently manipulated. In the multilayer case, we discover that the dopability has a close connection with the interlayer spacing. When the interlayer spacing is increased, the electron-doped $(CoO_2)^-$ layer undergoes a spontaneous overflow of electrons, which forms interlayer conducting channels. These free-electron-like states are reminiscent of the widely studied superconducting GIC. The predicted efficient tunability of both magnetic and electronic properties not only extends the applications of CoO_2 thin films to new territories but also sheds new light on the strong correlation effects long debated in CoO_2-based materials.

ASSOCIATED CONTENT

Supporting Information

The Supporting Information is available free of charge at https://pubs.acs.org/doi/10.1021/acs.jpcc.0c07847.

The structural data of CoO_2; the band structure of multilayer CoO_2 with different stacking orders; the phonon spectra and AIMD simulation results of monolayer CoO_2; the representative spin configurations in the $4 \times 2\sqrt{3}$ supercell and their relative energy; and the band gap evolution of monolayer CoO_2 with respect to spin configuration and U values (PDF)

AUTHOR INFORMATION

Corresponding Authors

Zheng Liu − *Institute for Advanced Study, Tsinghua University, Beijing 100084, China; State Key Laboratory of Low Dimensional Quantum Physics and Department of Physics, Beijing 100084, China*; Email: zheng-liu@tsinghua.edu.cn

Jian Wu − *State Key Laboratory of Low Dimensional Quantum Physics and Department of Physics, Beijing 100084, China*; Email: wu@phys.tsinghua.edu.cn

Shunhong Zhang − *International Center for Quantum Design of Functional Materials (ICQD), Hefei National Laboratory for Physical Sciences at the Microscale, and CAS Center For Excellence in Quantum Information and Quantum Physics, University of Science and Technology of China, Hefei, Anhui 230026, China*; orcid.org/0000-0003-2120-4574; Email: szhang2@ustc.edu.cn

Authors

Li Liang − *Institute for Advanced Study, Tsinghua University, Beijing 100084, China; State Key Laboratory of Low Dimensional Quantum Physics and Department of Physics, Beijing 100084, China; Institute of Electronic Engineering, China Academy of Engineering Physics, Mianyang 621999, China*

Shiqiao Du − *State Key Laboratory of Low Dimensional Quantum Physics and Department of Physics, Beijing 100084, China*

Lili Wang − *State Key Laboratory of Low Dimensional Quantum Physics and Department of Physics, Beijing 100084, China*

Complete contact information is available at: https://pubs.acs.org/10.1021/acs.jpcc.0c07847

Notes

The authors declare no competing financial interest.

https://dx.doi.org/10.1021/acs.jpcc.0c07847
J. Phys. Chem. C 2021, 125, 873−877

■ ACKNOWLEDGMENTS

This work was supported by the Tsinghua University Initiative Scientific Research Program and NSFC under Grant Nos. 11774196 and 11904350. S.Z. also acknowledges the support of the initiative program of USTC and Anhui Provincial Natural Science Foundation (Grant No. 2008085QA30).

■ REFERENCES

(1) Terasaki, I.; Sasago, Y.; Uchinokura, K. Large thermoelectric power in $NaCo_2O_4$ single crystals. *Phys. Rev. B* **1997**, *56*, R12685−R12687.
(2) Fujita, K.; Mochida, T.; Nakamura, K. High-temperature thermoelectric properties of $Na_xCoO_{2-\delta}$ single crystals. *Jpn. J. Appl. Phys.* **2001**, *40*, 4644−4647.
(3) Delmas, C.; Braconnier, J.-J.; Fouassier, C.; Hagenmuller, P. Electrochemical intercalation of sodium in Na_xCoO_2 bronzes. *Solid State Ionics* **1981**, *3-4*, 165−169.
(4) Shacklette, L. W.; Jow, T. R.; Townsend, L. Rechargeable electrodes from sodium cobalt bronzes. *J. Electrochem. Soc.* **1988**, *135*, 2669−2674.
(5) Wang, L.; Chen, B.; Ma, J.; Cui, G.; Chen, L. Reviving lithium cobalt oxide-based lithium secondary batteries-toward a higher energy density. *Chem. Soc. Rev.* **2018**, *47*, 6505−6602.
(6) Takada, K.; Sakurai, H.; Takayama-Muromachi, E.; Izumi, F.; Dilanian, R. A.; Sasaki, T. Superconductivity in two-dimensional CoO_2 layers. *Nature* **2003**, *422*, 53−55.
(7) Sugiyama, J.; Brewer, J. H.; Ansaldo, E. J.; Itahara, H.; Tani, T.; Mikami, M.; Mori, Y.; Sasaki, T.; Hébert, S.; Maignan, A. Dome-shaped magnetic phase diagram of thermoelectric layered cobaltites. *Phys. Rev. Lett.* **2004**, *92*, No. 017602.
(8) Foo, M. L.; Wang, Y.; Watauchi, S.; Zandbergen, H. W.; He, T.; Cava, R. J.; Ong, N. P. Charge ordering, commensurability, and metallicity in the phase diagram of the layered Na_xCoO_2. *Phys. Rev. Lett.* **2004**, *92*, No. 247001.
(9) Lang, G.; Bobroff, J.; Alloul, H.; Collin, G.; Blanchard, N. Spin correlations and cobalt charge states: Phase diagram of sodium cobaltates. *Phys. Rev. B* **2008**, *78*, No. 155116.
(10) Zhang, P.; Luo, W.; Crespi, V. H.; Cohen, M. L.; Louie, S. G. Doping effects on the electronic and structural properties of CoO_2: An LSDA + U study. *Phys. Rev. B* **2004**, *70*, No. 085108.
(11) Zhang, P.; Luo, W.; Cohen, M. L.; Louie, S. G. Fermi surface of Na_xCoO_2. *Phys. Rev. Lett.* **2004**, *93*, No. 236402.
(12) Sugiyama, J.; Brewer, J. H.; Ansaldo, E. J.; Hitti, B.; Mikami, M.; Mori, Y.; Sasaki, T. Electron correlation in the two-dimensional triangle lattice of Na_xCoO_2. *Phys. Rev. B* **2004**, *69*, No. 214423.
(13) Wang, G.-T.; Dai, X.; Fang, Z. Phase diagram of Na_xCoO_2 studied by Gutzwiller density-functional theory. *Phys. Rev. Lett.* **2008**, *101*, No. 066403.
(14) Zhong, Y.; et al. Nodeless pairing in superconducting copper-oxide monolayer films on $Bi_2Sr_2CaCu_2O_{8+\delta}$. *Sci. Bull.* **2016**, *61*, 1239−1247.
(15) Zhong, Y.; Fan, J.-Q.; Wang, R.-F.; Wang, S.; Zhang, X.; Zhu, Y.; Dou, Z.; Yu, X.-Q.; Wang, Y.; Zhang, D.; Zhu, J.; Song, C.-L.; Ma, X.-C.; Xue, Q.-K. Direct Visualization of Ambipolar Mott Transition in Cuprate CuO_2 Planes. *Phys. Rev. Lett.* **2020**, *125*, No. 077002.
(16) Wang, Q.-Y.; et al. Interface-induced high-temperature superconductivity in single unit-cell FeSe Films on $SrTiO_3$. *Chin. Phys. Lett.* **2012**, *29*, No. 037402.
(17) Wu, R.; Wang, L. et al. unpublished.
(18) Venimadhav, A.; Soukiassian, A.; Tenne, D. A.; Li, Q.; Xi, X. X.; Schlom, D. G.; Arroyave, R.; Liu, Z. K.; Sun, H. P.; Pan, X.; Lee, M.; Ong, N. P. Structural and transport properties of epitaxial Na_xCoOZ_2 thin films. *Appl. Phys. Lett.* **2005**, *87*, No. 172104.
(19) Kresse, G.; Furthmüller, J. Efficient iterative schemes for ab initio total-energy calculations using a plane-wave basis set. *Phys. Rev. B* **1996**, *54*, 11169−11186.
(20) Blöchl, P. E. Projector augmented-wave method. *Phys. Rev. B* **1994**, *50*, 17953−17979.
(21) Perdew, J. P.; Burke, K.; Ernzerhof, M. Generalized gradient approximation made simple. *Phys. Rev. Lett.* **1996**, *77*, 3865−3868.
(22) Dudarev, S. L.; Botton, G. A.; Savrasov, S. Y.; Humphreys, C. J.; Sutton, A. P. Electron-energy-loss spectra and the structural stability of nickel oxide: An LSDA+U study. *Phys. Rev. B* **1998**, *57*, 1505−1509.
(23) Amatucci, G. G.; Tarascon, J. M.; Klein, L. C. CoO2, The End Member of the Li x CoO2 Solid Solution. *J. Electrochem. Soc.* **1996**, *143*, 1114−1123.
(24) Takada, K.; Sakurai, H.; Takayama-Muromachi, E.; Izumi, F.; Dilanian, R. A.; Sasaki, T. Influences of interlayer distance and cobalt oxidation state on superconductivity of NaxCoO2. *Phys. C* **2004**, *412-414*, 14−20. Proceedings of the 16th International Symposium on Superconductivity (ISS 2003). Advances in Superconductivity XVI. Part I.
(25) Takada, K.; Sakurai, H.; Takayama-Muromachi, E.; Izumi, F.; Dilanian, R.; Sasaki, T. A New Superconducting Phase of Sodium Cobalt Oxide. *Adv. Mater.* **2004**, *16*, 1901−1905.
(26) Kawasaki, S.; Motohashi, T.; Shimada, K.; Ono, T.; Kanno, R.; Karppinen, M.; Yamauchi, H.; Zheng, G.-q. Measurement of electron correlations in Li_xCoO_2 (x = 0.0 −0.35) using ^{59}Co nuclear magnetic resonance and nuclear quadrupole resonance techniques. *Phys. Rev. B* **2009**, *79*, No. 220514.
(27) Ishida, H.; Johannes, M. D.; Liebsch, A. Effect of dynamical coulomb correlations on the fermi surface of $Na_{0.3}CoO_2$. *Phys. Rev. Lett.* **2005**, *94*, No. 196401.
(28) Boehnke, L.; Lechermann, F. Getting back to Na_xCoO_2: Spectral and thermoelectric properties. *Phys. Status Solidi A* **2014**, *211*, 1267−1272.
(29) Cococcioni, M.; de Gironcoli, S. Linear response approach to the calculation of the effective interaction parameters in the LDA + U method. *Phys. Rev. B* **2005**, *71*, No. 035105.
(30) Ye, Z. R.; Zhang, Y.; Chen, F.; Xu, M.; Jiang, J.; Niu, X. H.; Wen, C. H. P.; Xing, L. Y.; Wang, X. C.; Jin, C. Q.; Xie, B. P.; Feng, D. L. Extraordinary doping effects on quasiparticle scattering and bandwidth in Iron-based superconductors. *Phys. Rev. X* **2014**, *4*, No. 031041.
(31) Razzoli, E.; et al. Tuning electronic correlations in transition metal pnictides: Chemistry beyond the valence count. *Phys. Rev. B* **2015**, *91*, No. 214502.
(32) Lee, K.; Kim, S. W.; Toda, Y.; Matsuishi, S.; Hosono, H. Dicalcium nitride as a two-dimensional electride with an anionic electron layer. *Nature* **2013**, *494*, 336−340.
(33) Zhao, S.; Li, Z.; Yang, J. Obtaining two-dimensional electron gas in free space without resorting to electron doping: An electride based design. *J. Am. Chem. Soc.* **2014**, *136*, 13313−13318.
(34) Weller, T. E.; Ellerby, M.; Saxena, S. S.; Smith, R. P.; Skipper, N. T. Superconductivity in the intercalated graphite compounds C_6Yb and C_6Ca. *Nat. Phys.* **2005**, *1*, 39−41.
(35) Csányi, G.; Littlewood, P. B.; Nevidomskyy, A. H.; Pickard, C. J.; Simons, B. D. The role of the interlayer state in the electronic structure of superconducting graphite intercalated compounds. *Nat. Phys.* **2005**, *1*, 42−45.

https://dx.doi.org/10.1021/acs.jpcc.0c07847
J. Phys. Chem. C 2021, 125, 873−877